Received: 3 September 2022 | Accepted: 2 December 2022

DOI: 10.1002/ame2.12303

ORIGINAL ARTICLE

A new method for preparing a rat intracerebral hemorrhage model by combining focused ultrasound and microbubbles

Yao He[1] | Jie Yang[2] | Fengying Hu[3] | Min Liao[2] | Yuru Nie[3] | Xiaoxia Zhu[2] | Tao Zhang[4] | Keer Song[5] | Qinxi Li[1] | Xiaojie Li[1] | Chenghan Mei[1] | Zhe Wu[3] | Qiang Lu[2] | Zhihui Zhong[1]

[1]Laboratory of Nonhuman Primate Disease Modeling Research, State Key Laboratory of Biotherapy, West China Hospital, Sichuan University, Chengdu, China

[2]Department of Medical Ultrasound, West China Hospital, Sichuan University, Chengdu, China

[3]School of Life Science and Technology, University of Electronic Science and Technology of China, Chengdu, China

[4]School of Bioscience and Technology, Chengdu Medical College, Chengdu, China

[5]Franklin College of Arts and Science, University of Georgia, Athens, Georgia, USA

Correspondence
Zhe Wu, School of Life Science and Technology, University of Electronic Science and Technology of China, Chengdu, China.
Email: wuzhe@uestc.edu.cn

Qiang Lu, Department of Medical Ultrasound, West China Hospital, Sichuan University, Chengdu, China.
Email: luqiang@scu.edu.cn

Zhihui Zhong, Laboratory of Nonhuman Primate Disease Modeling Research, State Key Laboratory of Biotherapy, West China Hospital, Sichuan University, Chengdu, China.
Email: zhongzhihui@scu.edu.cn

Funding information
National Natural Scientific Foundation of China (82071349, 82027808, 82171952, 81771310) and West China Hospital of Sichuan University Discipline Excellence Development 1·3·5 Engineering Project (Interdisciplinary Innovation Project, ZYYC08005, ZYJC18041).

Abstract

Background: We aimed to prepare a non-invasive, reproducible, and controllable rat model of intracerebral hemorrhage with focused ultrasound (FUS).

Methods: A rat intracerebral hemorrhage (ICH) model was established by combining FUS and microbubbles (μBs), and edaravone was used to verify whether the free radical scavenger had a protective effect on the model. The brain tissue of each group was sectioned to observe the gross histology, blood–brain barrier (BBB) permeability, cerebral infarction volume, and histopathological changes.

Results: Compared with the FUS group, the BBB permeability was significantly increased in the FUS+μBs (F&B) group ($p = 0.0021$). The second coronal slice in the F&B group had an obvious hemorrhage lesion, and the FUS+μBs+edaravone (F&B&E) group had smaller hemorrhage areas; however, ICH did not occur in the FUS group. The cerebral infarction volume in the F&B group was significantly larger than that in the FUS group ($p = 0.0030$) and F&B&E group ($p = 0.0208$). HE staining results showed that nerve fibrinolysis, neuronal necrosis, microglia production, and erythrocytes were found in both the F&B group and the F&B&E group, but the areas of the nerve fibrinolysis and neuronal necrosis in the F&B group were larger than the F&B&E group.

Conclusions: A rat ICH model was successfully prepared using the μBs assisted FUS treatment, and edaravone had a therapeutic effect on this model. This model can be used to study the pathophysiological mechanism of ICH-related diseases and in preclinical research on related new drugs.

Yao He, Jie Yang, and Fengying Hu contributed equally to this work.

KEYWORDS
focused ultrasound (FUS), ICH model, microbubbles (μBs), rat

1 | INTRODUCTION

Intracerebral hemorrhage (ICH) is a common type of stroke (about 10%–15% of strokes) with high morbidity and mortality.[1–3] Most of the survivors have sequelae of varying degrees of motor impairment, cognitive impairment, and speech and swallowing disorders. The treatment of ICH patients involves the urgent treatment of mass effect, aggressive blood pressure reduction, and correction of contributing coagulopathies to achieve hemostasis and keep the patient stabilized.[4] However, few ICH patients benefit from existing therapies.[5] Effective treatments for ICH patients are desperately needed and this depends on appropriate animal models.

An ideal animal model mimics the natural events of hemorrhagic stroke in human beings. Rodent, canine, feline, and primate models of ICH, using mechanical balloon compression, bacterial collagenase, and either donor or autologous blood injection, have been reported in the past.[6–8] These models have been used to study different pathophysiological aspects of ICH and its clinical disease progression. However, some inevitable disadvantages are noted. Mechanical balloon compression cannot naturally model the spontaneous hemorrhage progress and the ICH associated pathophysiologic changes. Consequently, this method has little application.[8] The external injection methods are widely acceptable but invasive, which can lead to untargeted brain parenchyma injury and extra inflammation.[9] Hence, it is necessary to establish a non-invasive, reproducible, and stable animal model of spontaneous intracerebral hemorrhage.

SonoVue (sulfur hexafluoride microbubble (μBs) for injection, Bracco Diagnostics Inc., Milan, Italy), a pure blood pool agent, is currently a widely used ultrasound contrast agent. It is commercially available and clinically approved for disease diagnosis,[10] with low solubility in blood; it is also non-toxic.[11] SonoVue is a second-generation contrast agent composed of a sulfur hexafluoride core and a phospholipid coating. μBs are used as contrast enhancers in ultrasound imaging, drug/gene delivery vectors, thrombus reducers, oxygen gas carriers, and drug delivery across the BBB.[12]

Focused ultrasound (FUS) has been widely used as a non-invasive ablation technique with millimeter-sized focal regions for the destruction of tissue without disruption of surrounding tissue by either thermal or mechanical bio-effects.[13] FUS has been applied to generate mechanical bioeffects by co-administering μBs to trigger the acoustic cavitation effect.[14] With the application of sufficient acoustic pressure (>100 kPa), the μBs generate nonlinear oscillations, leading to non-inertial and/or inertial cavitation, which can produce significant microstreaming.[15] This bioeffect can lead to cellular injury or tissue destruction and is reported to be helpful in the treatment of tumors,[16,17] immunotherapy,[18] BBB opening,[19–21] and drug delivery.[22]

We were thus inspired to hypothesize that when μBs and FUS are co-administered at a desired region within the rats' brain, local spontaneous ICH may occur due to the vessel rupturing cavitation bioeffect. Therefore, this study aimed to introduce a non-invasive and reproducible ICH model in rats by using FUS with μBs and to delineate changes in neurologic outcome and histology in acute ICH conditions.

2 | METHODS

2.1 | Experimental animals

Thirty-three Sprague Dawley (SD) male rats (age 6–7 weeks, weight 200–250 g) were purchased from Beijing Vital River Laboratory Animal Technology Co., Ltd. The animals were housed under specific pathogen-free (SPF) conditions, at 22 ± 2°C and 55 ± 10% relative humidity, with a 12 h light/dark cycle. We randomly divided thirty rats into three experimental groups using a random number table based on body weight. Six rats were treated with FUS without injection of μB (FUS group), fourteen were treated with FUS and injection of μBs (FUS + μBs group, F&B group), and ten were treated with FUS, injection of μBs and 6.0 mg/kg edaravone (FUS + μBs + Edaravone group, F&B&E group). Neither μBs nor FUS intervention was given to three rats (Sham group), and the remaining operations were consistent with those of the other groups. The protocols were approved by the Institutional Animal Care and Use Committee (IACUC) of West China Hospital, Sichuan University (Approval No. 2019192A). All animals were acclimated to the laboratory for 1 week.

2.2 | Acoustic setups

An Agilent N9310A RF Signal Generator (Agilent Technology Co., Ltd, Santa Clara, USA) was used to generate the driving signals. The signals were tone burst sine waves at 1.1 MHz with a 20% duty cycle and a 200 Hz pulse repetition rate. The signals were subsequently amplified by an ENI Model 3100LA RF Power Amplifier (Rochester, USA). The amplified signal was transmitted to the transducer via an impedance matching network (Sonic Concepts Inc., Bothell, USA) which was set to its fundamental mode. An H102 transducer from Sonic Concepts fitted with a customized focusing cone directed the ultrasonic energy to the rat's head, forming an oval-shaped acoustic focus at 5 mm beneath the skull surface. The schematic of the acoustic setup is shown in Figure 1A.

2.3 | Marking the target site

Rats were fasted for 10 h before surgery and anesthetized with isoflurane mixed with oxygen (5% for surgical induction, 2% to

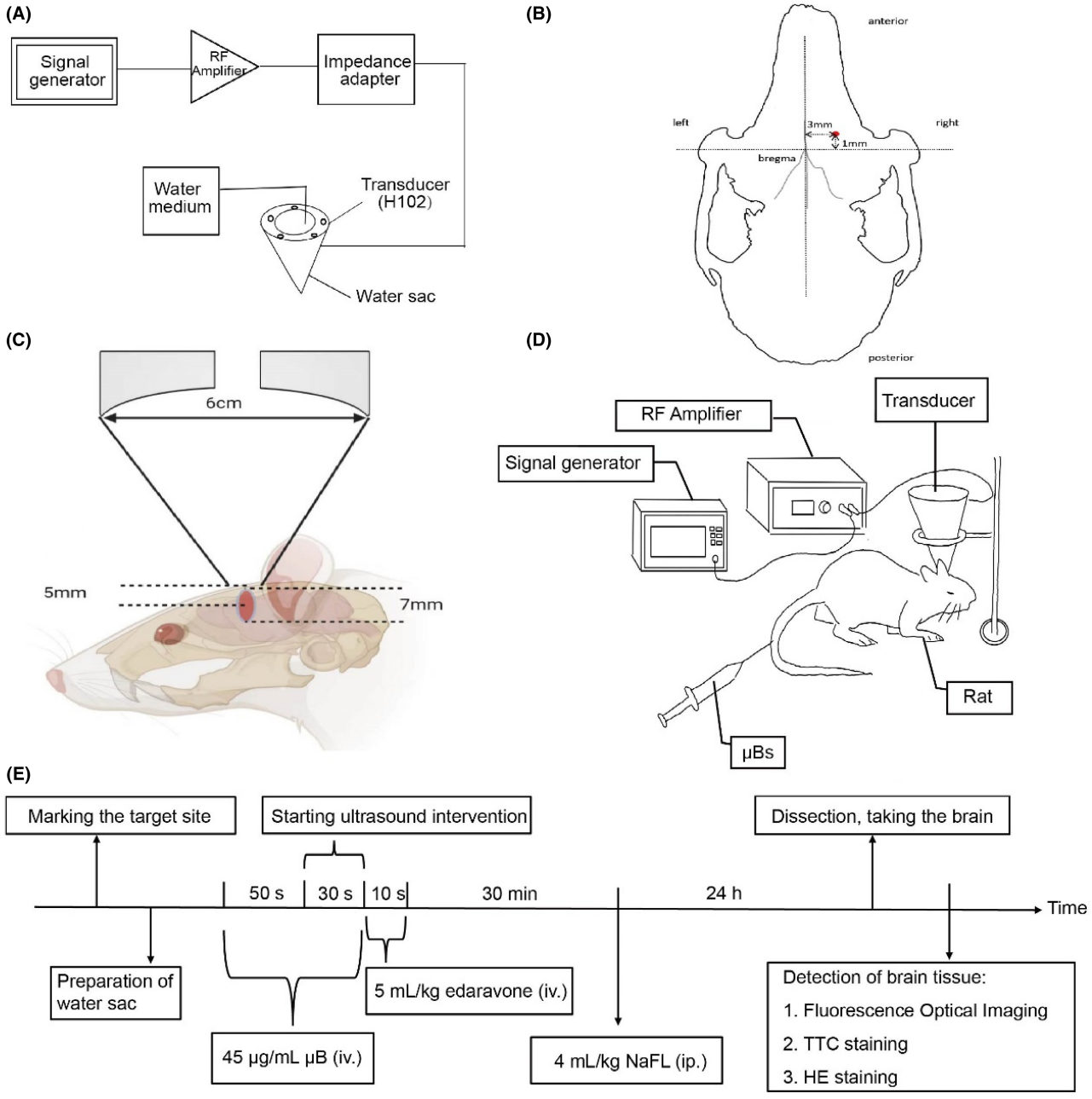

FIGURE 1 (A) The connections of the device. (B) A plane diagram of the target site for ultrasound intervention. (C) A schematic image representing the target coordinates of FUS. (D) Schematic diagram of the intervention procedure. (E) Experimental timeline.

2.5% for maintenance). After anesthesia, the rats were fixed in a stereotaxic apparatus. The cranial skin was sterilized and split, and then 3% hydrogen peroxide was used to uncover the periosteum, thus exposing the bregma of the skull. The anterior bregma was used as a point to mark the target site. According to the stereoscopic map of the rat brain, we identified the striatum as the target site of focused ultrasound. The coordinates were 3.0 mm right, 1.0 mm anterior, and 5.0 mm ventral from bregma at the skull surface using a stereotactic apparatus. The schematic image that represents the target coordinates of FUS is shown in Figure 1B,C.

2.4 | Preparation of water sac and turning on the device

The bottom of the transducer was wrapped with plastic wrap, and the transducer was filled with pure water to form a water sac, which was then aligned to the marked position on the head of rat. After that, an ultrasonic coupling agent was applied between the adventitia of the water sac and the skull to make a tight connection.

With the help of a microinjection pump, all groups except for the FUS group were injected with 45 μg/ml of μBs (SonoVue®) via the tail vein of the rats, at an injection speed of 5 μl/s. The injection of

μBs took a total of 80 s. The first 50 s were used to stabilize the concentration of μBs in the blood pool (0.8–1.0 ml/kg), and during the last 30 s the equipment was activated for ultrasound intervention. The parameters of the ultrasonic equipment are shown in Table 1. After ultrasound intervention, the rats in the F&B&E group were immediately injected with edaravone (6 mg/kg) via the tail vein. Thirty minutes after the ultrasound intervention, rats in each group were intraperitoneally injected with 10% sodium fluorescein (NaFL) at a dose of 4 ml/kg.

2.5 | Detection of BBB permeability, cerebral infarction volume, and morphological structure of brain tissue

Twenty-four hours post ultrasound intervention, the rats were anesthetized with 3% pentobarbital sodium. The rat hearts were perfused with PBS solution, and the brain tissue was removed and observed for gross histology, especially at the ICH location. The number of red pixels in the gross histology was counted as a rough quantification of the hemorrhage. Subsequently, the brain tissue was cut into six coronal slices of 2 mm thickness. The slices underwent the following fluorescent imaging and the TTC staining for side-by-side comparison. BBB permeability was detected using the fluorescence imaging mode of an IVIS® Lumia series III imaging system (PerkinElmer, USA), and fluorescence intensity was quantized using the total radiant efficiency (TRE) value. The fluorescence imaging methods were detailed in our previous study.[23] The same brain slices were subsequently stained with 2,3,5-triphenyl tetrazolium chloride (TTC), and the cerebral infarction volume of each group was analyzed with ImageJ software (National Institutes of Health, Bethesda, USA). Two brain tissue samples were randomly selected from the F&B group and the F&B&E group for HE staining to observe the morphological structure of the hemorrhagic area of the brain tissue. A schematic diagram of the intervention procedure and the experimental timeline are shown in Figure 1D,E.

2.6 | Statistical analysis

GraphPad Prism software (GraphPad Software Inc., San Diego, USA) version 9.0 was used for statistical analysis. Gaussian distributed data (Shapiro–Wilk test) were expressed as means ± standard deviation (mean ± SD). The TRE in each group was evaluated for statistical significance by the nonparametric Mann–Whitney test. Comparison of cerebral infarction volumes among groups was tested by the unpaired *t* test. *p* values <0.05 were considered statistically significant.

3 | RESULTS

3.1 | Successfully established rat ICH model by FUS

In our research, none of the animals in any group died during the experiment. The mortality rate was zero. In addition, hematoma lesions were observed in all rats in the F&B group. In other words, the success rate of establishing the rat ICH model with our new method is 100%. In the F&B&E group, no hematoma lesions were observed in two rats, while hematoma was found in the remaining rats, but the size of the hematoma was smaller than that in the F&B group.

TRE values were $3.23 \pm 0.66 \times 10^{10}$ in the Sham group, $3.65 \pm 0.92 \times 10^{10}$ in the FUS group, and $1.55 \pm 0.88 \times 10^{11}$ in the F&B group. As shown in Figure 2A, BBB permeability was slightly increased in the FUS group compared with the Sham group. Compared to the FUS group, the BBB permeability was significantly enhanced in F&B group (Figure 2A,B, $P = 0.0021$). It can be seen from the coronal brain slices in Figure 2C that no cerebral hemorrhage symptoms occurred in the FUS group, while cerebral hemorrhage occurred in the F&B group, indicating that with the help of μBs, FUS can non-invasively create a rat ICH model. TTC staining showed no cerebral infarction in the sham group (Figure 2C). At the same time, the ratios of cerebral infarction volume to whole brain volume were 0.93% ± 0.67% in the FUS group and 3.13% ± 1.46% in the F&B group. The F&B group had a significantly larger cerebral infarction volume than that of the FUS group (Figure 2D, $p = 0.0030$). Since it is well known that hemorrhage causes excessive brain tissue damage,[4] it is reasonable to assume that the extra infarction volume was caused by the hemorrhage induced by ultrasound, further indicating that hemorrhagic cerebral infarction occurred in the F&B group. In particular, we noted that the fluorescent intensity distribution correlates

TABLE 1 Acoustic parameters of each group

	Parameter				
Group	Frequency (MHz)	Acoustic pressure (MPa)	Duty ratio (%)	Time (s)	Number
Sham	–	–	–	–	3
FUS	1.1	9	20	30	6
FUS + μBs (F&B)	1.1	9	20	30	14
FUS + μBs + Edaravone (F&B&E)	1.1	9	20	30	10

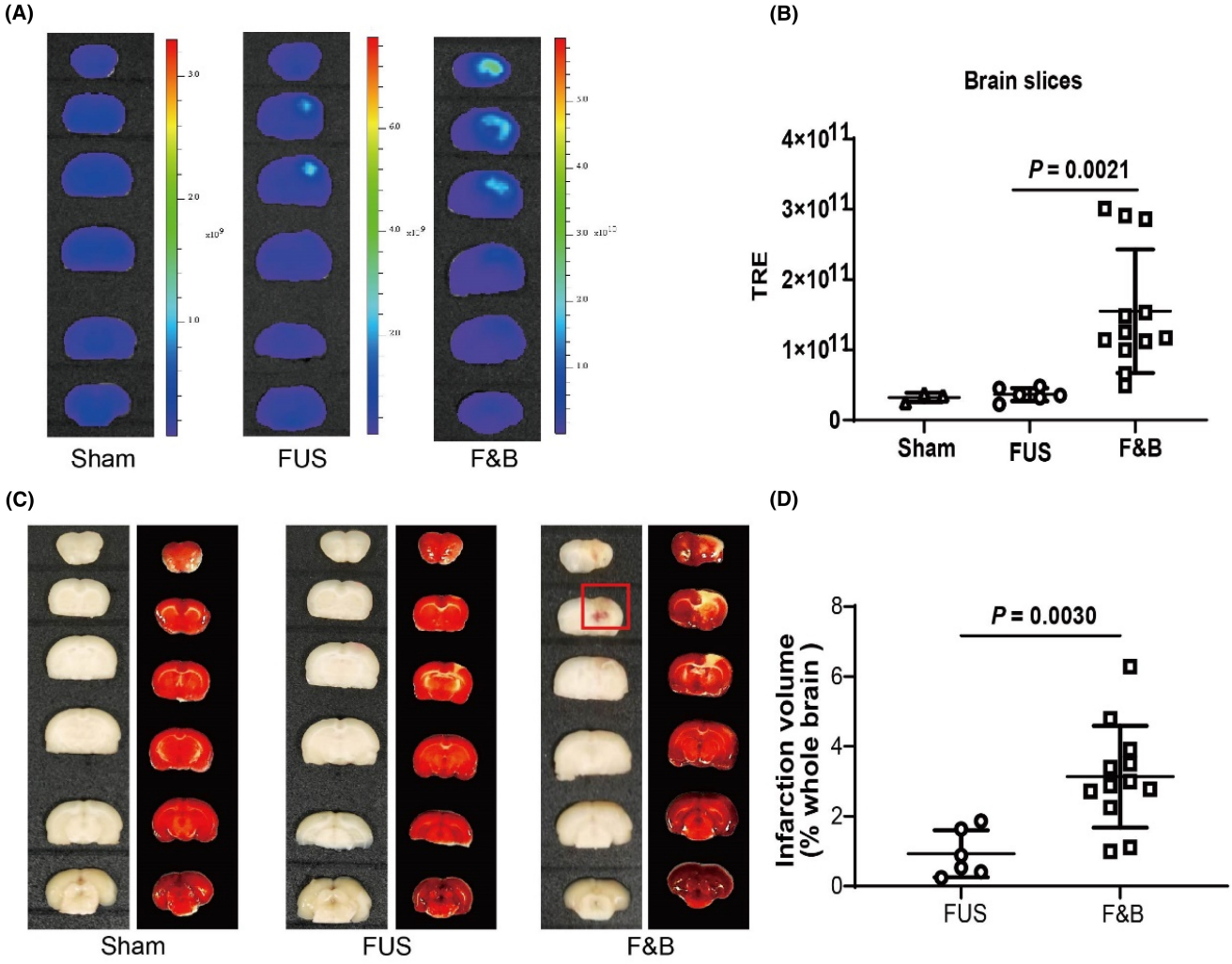

FIGURE 2 (A) Representative images of brain slices detected by the IVIS® Lumina III system in three groups. The relative fluorescence intensity is color graded as low (blue), medium (green), and high (red). (B) Quantification the fluorescence intensity of brain slices in three groups. (C) Representative images of brain slices before and after TTC staining in three groups. The red pixel in the red box is the cerebral hemorrhage lesion. (D) Cerebral infarction volume in two groups.

spatially with the tissue infarction location, in accordance with the ultrasound focus.

3.2 | Protective effect of edaravone on rat ICH model

In Figure 3A, the red-framed brain slices of the F&B group and F&B&E group had different degrees of hemorrhage. The cerebral infarction volume in the F&B&E group was 1.90%±0.78%, which was significantly smaller than that in F&B group (Figure 3B, $p = 0.0208$). It indicated that the therapeutic effect of edaravone reduced cerebral infarction volume.

The HE staining results (Figure 3C) of brain tissue showed that nerve fibrinolysis, neuronal necrosis, microglia production and erythrocytes were found in both groups, but the area of the nerve fibrinolysis in the F&B group was larger than that in the F&B&E group, indicating that edaravone can reduce the nerve fibrinolysis and has a therapeutic effect in this model.

4 | DISCUSSION

Microbubbles expand continuously when subjected to ultrasonic waves and rupture when the sound pressure reaches a certain value. In this process, the ultrasonic cavitation effect causes damage or even rupture of the blood vessel walls. Under the same acoustic conditions, the BBB permeability of the FUS group and the F&B group were both increased, but the BBB permeability of the latter was significantly greater than that of the former, which was consistent with existing reports that μBs contribute to the increase in BBB permeability.[24] BBB permeability is an important pathophysiological process during the stroke.[25,26] At the same time, no intracerebral hemorrhage occurred in the FUS group, but different degrees of

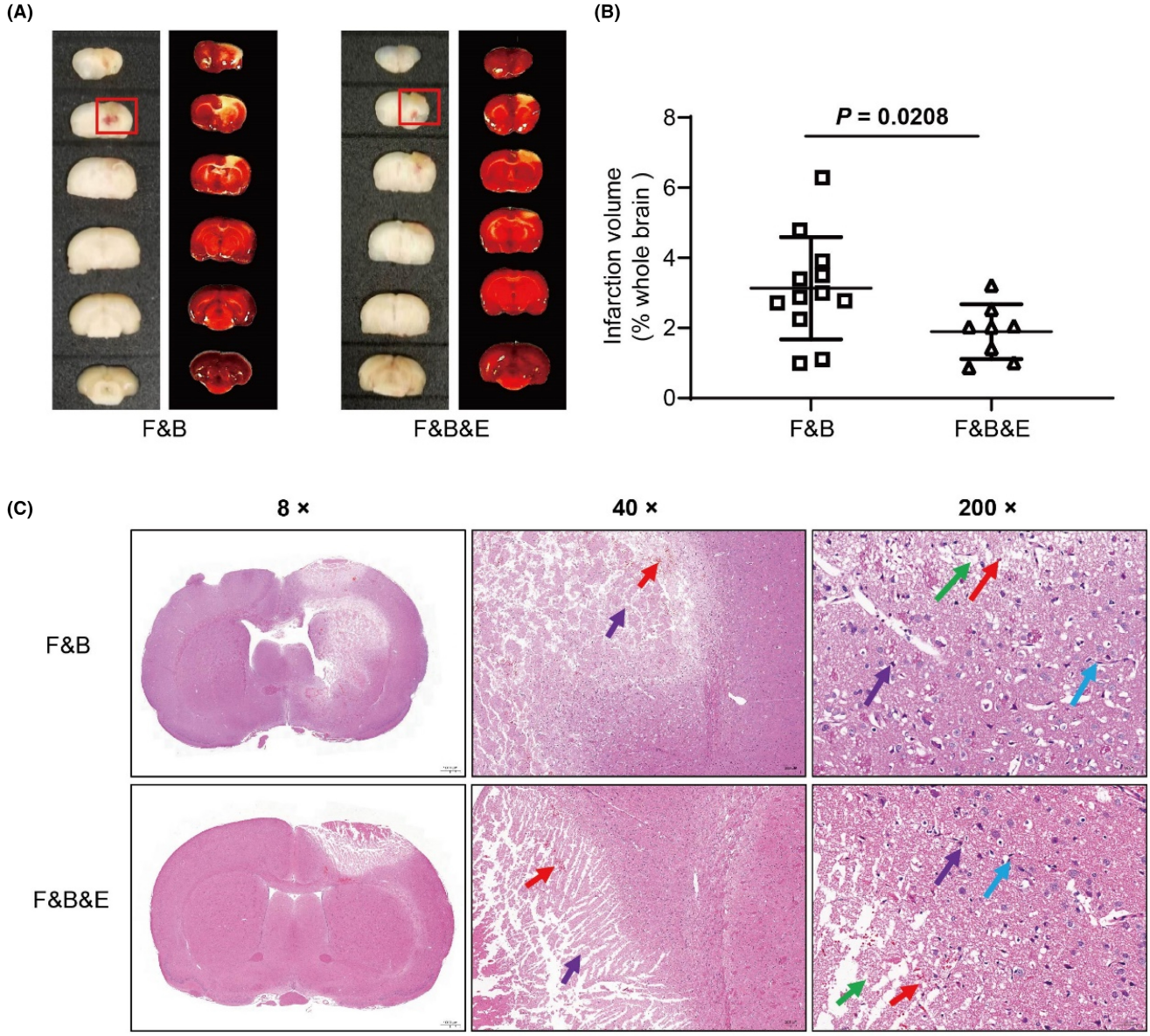

FIGURE 3 (A) Representative images of brain slices before and after TTC staining in two groups. The red pixel in the red box is the cerebral hemorrhage lesion. (B) Cerebral infarction volume in two groups. (C) Representative pictures of HE staining in two groups. Nerve fiber dissolution (green arrow), neuron necrosis (purple arrow), microglia (blue arrow), erythrocyte (red arrow). The corresponding HE stain results at different magnifications: 8× (bar = 1000 μm), 40× (bar = 200 μm), 200× (bar = 50 μm).

cerebral hemorrhage occurred when FUS and μBs are combined in the other two groups. Therefore, the presence of both the appropriate ultrasound field and the μBs are necessary for the hemorrhage to occur.

When ICH occurs, the hematoma compresses the surrounding tissue leading to ischemia and hypoxia in the compressed tissue, which causes oxidative stress and oxidative damage in the brain tissue.[27,28] Previous studies have shown that edaravone protects neurons and vascular endothelial cells by scavenging free radicals (such as hydrogen peroxide and hydroxyl radicals) and inhibiting lipid peroxidation.[29,30] Therefore, the reduced cerebral infarction volume in the F&B&E group is an indication that ICH indeed occurred in both μB-assisted FUS intervention groups. The results of HE staining showed that the areas of neuronal necrosis and nerve fibrinolysis in the edaravone treatment group were smaller than those in the group without the edaravone treatment, possibly because edaravone reduced the oxidative damage to the brain tissue and the local neurons were thus protected. This result indicates that μB-assisted FUS intervention not only successfully created a rat ICH model, but also that the cerebral infarction volume caused by the intervention can be improved by edaravone to some extent.

FUS has been used in the treatment of various solid tumors, such as liver cancer, breast cancer, prostate cancer, and malignant renal tumors.[31–33] The main mechanisms of FUS treatment of tumors are thermal and mechanical effects.[34] In our study, the ultrasound pulse sequence was designed to minimize the thermal effect. Moreover,

the cerebral blood flow carried away some of the thermal deposits. Nevertheless, the inevitable residual thermal effect may lead to additional damage to the brain tissue between the focal point and the transducer.[35] Because thermal damage is known to be irreversible, the portion of damage rescued with the edaravone therapy is proved to be nonthermal ICH. Hence, the cerebral infarct volume in this study consists of both the thermal effect-induced injury and the ICH-induced injury.

In follow-up studies, we will reduce the cerebral infarction volume caused by the thermal effect by adjusting the parameters of the device or preparing new μBs, and then optimize this model to make it a more reliable animal model for preclinical research of new drugs that treat spontaneous ICH-related diseases.

5 | CONCLUSION

This study reported a non-invasive, highly reproducible, and highly controllable rat ICH model prepared with μB-assisted FUS treatment. The ICH condition generated was found to be improved by the free radical scavenger edaravone, which may in future be used to explore the pathophysiological mechanisms of ICH-related diseases and in preclinical research into related new drugs. A residual thermal effect was documented and will be reduced in later research designs, such as by enhancing the maximum negative peak pressure of ultrasound or using improved nano-agents.

AUTHOR CONTRIBUTIONS

Zhihui Zhong, Qiang Lu, and Zhe Wu conceived the experiments. Yao He, Jie Yang, and Fengying Hu performed the experiments and drafted the manuscript. Min Liao, Yuru Nie, and Xiaoxia Zhu collected literature. Tao Zhang and Keer Song helped perform the analysis with constructive discussions. Qinxi Li, Xiaojie Li, and Chenghan Mei analyzed the data. All authors read and approved the final manuscript.

ACKNOWLEDGMENTS

This study was funded by the National Natural Scientific Foundation of China (82071349, 82027808, 82171952, 81771310) and West China Hospital of Sichuan University Discipline Excellence Development 1·3·5 Engineering Project (Interdisciplinary Innovation Project, ZYYC08005, ZYJC18041).

CONFLICT OF INTEREST

The authors have no competing interests to declare. Zhihui Zhong is an Editorial Board member of AMEM and a co-author of this article. To minimize bias, he was excluded from all editorial decision-making related to the acceptance of this article for publication.

ETHICS STATEMENT

The animal experiments were approved by the Institutional Animal Care and Use Committee (IACUC) of West China Hospital, Sichuan University (Approval No. 2019192A).

ORCID

Yao He https://orcid.org/0000-0002-4697-7250

Zhihui Zhong https://orcid.org/0000-0001-7892-9029

REFERENCES

1. Virani S, Alonso A, Benjamin EJ, et al. Heart disease and stroke statistics-2020 update: a report from the American Heart Association. *Circulation*. 2020;141(9):e139-e596.
2. Anderson C, Heeley E, Huang Y, et al. Rapid blood-pressure lowering in patients with acute intracerebral hemorrhage. *N Engl J Med*. 2013;368(25):2355-2365.
3. Li Y, Zhang J. Animal models of stroke. *Animal Model Exp Med*. 2021;4(3):204-219.
4. Schrag M, Kirshner H. Management of intracerebral hemorrhage: JACC focus seminar. *J Am Coll Cardiol*. 2020;75(15):1819-1831.
5. Woo D, Broderick J. Spontaneous intracerebral hemorrhage: epidemiology and clinical presentation. *Neurosurg Clin N Am*. 2002;13(3):265-279.
6. MacLellan C, Silasi G, Poon CC, et al. Intracerebral hemorrhage models in rat: comparing collagenase to blood infusion. *J Cereb Blood Flow Metab*. 2008;28(3):516-525.
7. Manaenko A, Chen H, Zhang JH, Tang J. Comparison of different preclinical models of intracerebral hemorrhage. *Acta Neurochir Suppl*. 2011;111:9-14.
8. Sinar EJ, Mendelow AD, Graham DI, Teasdale GM. Experimental intracerebral hemorrhage: effects of a temporary mass lesion. *J Neurosurg*. 1987;66(4):568-576.
9. Andaluz N, Zuccarello M, Wagner K. Experimental animal models of intracerebral hemorrhage. *Neurosurg Clin N Am*. 2002;13(3):385-393.
10. Nolsøe C, Lorentzen T. International guidelines for contrast-enhanced ultrasonography: ultrasound imaging in the new millennium. *Ultrasonography (Seoul, Korea)*. 2016;35(2):89-103.
11. Dindyal S, Kyriakides C. Ultrasound microbubble contrast and current clinical applications. *Recent Pat Cardiovasc Drug Discov*. 2011;6(1):27-41.
12. Upadhyay A, Dalvi S. Microbubble formulations: synthesis, stability, modeling and biomedical applications. *Ultrasound Med Biol*. 2019;45(2):301-343.
13. Hall TL, Hempel CR, Wojno K, Xu Z, Cain CA, Roberts WW. Histotripsy of the prostate: dose effects in a chronic canine model. *Urology*. 2009;74(4):932-937.
14. Stride E, Coussios C. Cavitation and contrast: the use of bubbles in ultrasound imaging and therapy. *Proc Inst Mech Eng H*. 2010;224(2):171-191.
15. Ho YJ, Li JP, Fan CH, Liu HL, Yeh CK. Ultrasound in tumor immunotherapy: current status and future developments. *J Control Release*. 2020;323:12-23.
16. Eisenbrey J, Forsberg F, Wessner CE, et al. US-triggered microbubble destruction for augmenting hepatocellular carcinoma response to transarterial radioembolization: a randomized pilot clinical trial. *Radiology*. 2021;298(2):450-457.
17. D'Souza J, Sultan LR, Hunt SJ, et al. Microbubble-enhanced ultrasound for the antivascular treatment and monitoring of hepatocellular carcinoma. *Nanotheranostics*. 2019;3(4):331-341.
18. Liu HL, Hsieh HY, Lu LA, Kang CW, Wu MF, Lin CY. Low-pressure pulsed focused ultrasound with microbubbles promotes an anticancer immunological response. *J Transl Med*. 2012;10:221.
19. Abrahao A, Meng Y, Llinas M, et al. First-in-human trial of blood-brain barrier opening in amyotrophic lateral sclerosis using MR-guided focused ultrasound. *Nat Commun*. 2019;10(1):4373.
20. Downs M, Buch A, Sierra C, et al. Long-term safety of repeated blood-brain barrier opening via focused ultrasound with microbubbles in non-human primates performing a cognitive task. *PLoS ONE*. 2015;10(5):e0125911.

21. Goutal S, Gerstenmayer M, Auvity S, et al. Physical blood-brain barrier disruption induced by focused ultrasound does not overcome the transporter-mediated efflux of erlotinib. *J Control Release*. 2018;292:210-220.
22. Kooiman K, Roovers S, Langeveld SAG, et al. Ultrasound-responsive cavitation nuclei for therapy and drug delivery. *Ultrasound Med Biol*. 2020;46(6):1296-1325.
23. He Y, Zhang Y, Li W, et al. Evaluating blood-brain barrier disruption and infarction volume concurrently in rats subjected to ischemic stroke using an optical imaging system. *J Neurosci Methods*. 2022;378:109630.
24. Choi JJ, Feshitan JA, Baseri B, et al. Microbubble-size dependence of focused ultrasound-induced blood-brain barrier opening in mice in vivo. *IEEE Trans Biomed Eng*. 2010;57(1):145-154.
25. Zhang Y, Fan F, Zeng G, et al. Temporal analysis of blood-brain barrier disruption and cerebrospinal fluid matrix metalloproteinases in rhesus monkeys subjected to transient ischemic stroke. *J Cereb Blood Flow Metab*. 2017;37(8):2963-2974.
26. Zhang Y, Zhao B, Lai Q, et al. Chronic cerebral hypoperfusion and blood-brain barrier disruption in uninjured brain areas of rhesus monkeys subjected to transient ischemic stroke. *J Cereb Blood Flow Metab*. 2022;42(7):1335-1346.
27. Zhang Y, Yang Y, Zhang GZ, et al. Stereotactic administration of edaravone ameliorates collagenase-induced intracerebral hemorrhage in rat. *CNS Neurosci Ther*. 2016;22(10):824-835.
28. Shang H, Cui D, Yang D, Liang S, Zhang W, Zhao W. The radical scavenger edaravone improves neurologic function and perihematomal glucose metabolism after acute intracerebral hemorrhage. *J Stroke Cerebrovasc Dis*. 2015;24(1):215-222.
29. Watanabe T, Yuki S, Egawa M, Nishi H. Protective effects of MCI-186 on cerebral ischemia: possible involvement of free radical scavenging and antioxidant actions. *J Pharmacol Exp Ther*. 1994;268(3):1597-1604.
30. Narayan SK, Grace Cherian S, Babu Phaniti P, Babu Chidambaram S, Rachel Vasanthi AH, Arumugam M. Preclinical animal studies in ischemic stroke: challenges and some solutions. *Animal Model Exp Med*. 2021;4(2):104-115.
31. Illing R, Kennedy JE, Wu F, et al. The safety and feasibility of extracorporeal high-intensity focused ultrasound (HIFU) for the treatment of liver and kidney tumours in a Western population. *Br J Cancer*. 2005;93(8):890-895.
32. Xu G, Luo G, He L, et al. Follow-up of high-intensity focused ultrasound treatment for patients with hepatocellular carcinoma. *Ultrasound Med Biol*. 2011;37(12):1993-1999.
33. Leslie T, Ritchie R, Illing R, et al. High-intensity focused ultrasound treatment of liver tumours: post-treatment MRI correlates well with intra-operative estimates of treatment volume. *Br J Radiol*. 2012;85(1018):1363-1370.
34. Dubinsky T, Cuevas C, Dighe MK, Kolokythas O, Hwang JH. High-intensity focused ultrasound: current potential and oncologic applications. *AJR Am J Roentgenol*. 2008;190(1):191-199.
35. Peng S, Zhou P, He W, Liao M, Chen L, Ma CM. Treatment of hepatic tumors by thermal versus mechanical effects of pulsed high intensity focused ultrasound in vivo. *Phys Med Biol*. 2016;61(18):6754-6769.

How to cite this article: He Y, Yang J, Hu F, et al. A new method for preparing a rat intracerebral hemorrhage model by combining focused ultrasound and microbubbles. *Anim Models Exp Med*. 2023;6:103-110. doi:10.1002/ame2.12303